International Journal of Enhanced Research in Science, Technology & Engineering
ISSN: 2319-7463, Vol. 5 Issue 3, March-2016

Influence of fluid rheology on the piston cylinder oil film development and pressure distribution considering medium speed effects in initial engine start up

Usman Chaudhri, Kendrick Aung

Department of Mechanical Engineering, Lamar University, Texas, USA

ABSTRACT

This paper investigates friction and wear between piston and cylinder liner during idling conditions with no or very little applied load. A 2-Dimensional non-Newtonian piston skirt lubrication model and analysis at the time of engine start up is presented. The well-established Maxwell model has been used to describe viscoelasticity encountered during the initial engine start up conditions. The analysis of lubricant rheology between piston and cylinder liner using characteristic lubricant relaxation times in all order of magnitude analysis is done by using the perturbation method. At low to medium engine start up speeds, the effects of viscoelasticity on lubricant velocity and pressure fields are examined and the influence of film thickness on lubricant characteristics is investigated. Numerical simulations show that piston eccentricities, hydrodynamic pressures, and film thickness profiles are strongly influenced by low to medium engine start up speeds.

Keywords: Engines, Lubrication, Non-Newtonian, Rheology, Friction, Wear.

1. INTRODUCTION

Initial engine start up is a critical phase for lubrication because less amount of engine oil is present and there exists a large piston to bore radial clearance. The initial start up of automobile engines covers the preliminary low to medium engine speeds prior to engine warm up at medium to high engine speeds. However, modern automotive vehicles starts out at high engine speeds in order to achieve the stable situation without delays, but these high operating speeds invite start up adhesive wear among interacting piston skirts and liner surfaces in the absence of lubricating oil film. With the evolution of advanced machine elements that experience severe operating conditions, the increasing use of non-Newtonian fluids during engine start up conditions have been emphasized. The viscosity index improvers in the engine lubricants enhance the performance of base stocks for different conditions of crucial engine operations [1]. The lubricant's viscosity should prevent start up wear and at the same time its mobility should facilitate smooth engine start up under the normal temperature conditions. In the past, Sinh law based Ree-Eyring type lubricant focusing on shear thinning effects was modeled even though there were evidence that suggested that such characteristics could not truly be modeled by that law [2]. Some researchers neglected the viscoelastic effects in compression and in shear while employing the thermal non-Newtonian Ree-Eyring lubrication model [3]. The non-Newtonian behavior of engine oils was modeled using various techniques. However, the attention of many researchers has been centered on the viscoelastic behavior of oils [4]. Newtonian fluid flow between the interacting surfaces in relative motion causes shearing of layers and contributes towards an increase in the energy dissipation. While in a viscoelastic model, energy storage is characterized by lubricant elasticity and energy dissipation as lubricant viscous effects. Maxwell type viscoelastic fluid flow model between the opposing surfaces facilitates reduction in energy dissipation [5].

2. OBJECTIVE

This study develops a viscoelastic hydrodynamic lubrication model at the initial engine start up speeds of 1000 rpm, 1500 rpm, and 2000 rpm. Numerical simulations will be conducted to investigate the impact of low to medium engine start up speeds (1000 – 2000 rpm) on piston eccentricities, hydrodynamic pressures, and film thickness profiles. In this study the following assumptions are considered in mathematical modeling of the problem [6].

1. Laminar flow
2. Turbulent effects are neglected.

3. Leakage at the sides and edges is neglected.
4. Pressure at the inlet zone is zero.
5. Lubricant is incompressible.
6. Thermal effects are neglected.
7. Surface roughness and waviness are neglected.
8. Squeeze and cavitation effects are neglected.

3. MATHEMATICAL MODEL

Piston and cylinder bore are two components of the power cylinder system. The chemical energy in the fuel is converted into kinetic energy during combustion and transmitted from the combustion chamber, through the piston, pin and connecting rod to the crank shaft. The geometric placement of the power cylinder system allows the linear motion of the piston to be converted into rotational motion of the crank shaft. The angle of the connecting rod causes lateral motion of the piston, and interaction with the bore, combined with lateral motion and friction at the wrist pin bearing tends to cause piston tilt as shown in Fig. 1.

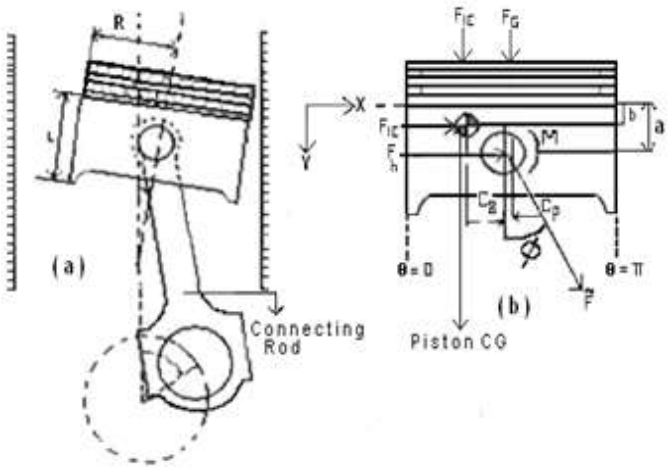

Figure 1 Schematic of Piston Cylinder System (a) and (b) [7]

The symbols used in Fig. 1 are explained below in Table 1.

Table 1. Nomenclature of Fig. 1

Symbol	Description
a	Vertical distance from skirt top to the piston-pin
b	Vertical distance from skirt top to piston center of gravity
C	Radial clearance between piston and cylinder bore
C_g	Horizontal distance between piston center of mass and piston pin
C_p	Horizontal distance of the piston-pin from the axis of piston
F	Normal force acting on piston skirts
F_f	Friction force acting on skirt surface
F_g	Gas force
F_{IC}	Inertia force due to piston mass
F_{IP}	Inertia force due to piston pin mass
L	Piston skirt length
M	Moment acting on piston skirts
R	Radius of piston
Φ	Connecting rod angle
Ψ, θ, x	Crank angle

Table 2 shows the input parameters that are used in all simulations reported in this paper.

Table 2. Input parameters for piston geometry [5]

No.	Parameter	Value	No.	Parameter	Value
1	Length a	12.5 mm	6	Pin offset	1 mm

2	Length b	15 mm	7	Clearance	0.01 mm
3	Mass of pin, m_{pin}	0.09 kg	8	Crank	41.8 mm
4	Mass of piston, m_{pis}	0.295 kg	9	Piston radius, R	41.5 mm
5	Skirt length, L	33.8 mm	10	Connecting rod, l	133 mm

Apart from the primary piston axial motion, its small secondary transverse eccentric displacements along the direction perpendicular to the axis of cylinder known as piston slap are incorporated in the equations of piston motion. Piston skirt eccentricities at the skirt top (Et) and bottom (Eb) are calculated by considering piston inertia, hydrodynamic force, hydrodynamic friction force, and moments in the form of (1) similar to that defined by Zhu et al. [7].

$$\begin{bmatrix} m_{pis}\left(1-\frac{a}{L}\right)+m_{pis}\left(1-\frac{b}{L}\right) & m_{pis}\frac{a}{L}+m_{pis}\frac{b}{L} \\ \frac{I_{pis}}{L}+m_{pis}(a-b)\left(1-\frac{b}{L}\right) & m_{pis}(a-b)\frac{b}{L}-\frac{I_{pis}}{L} \end{bmatrix}\begin{bmatrix} \ddot{e}_t \\ \ddot{e}_b \end{bmatrix}=\begin{bmatrix} F_h+F_s+F_{fh}\tan\Phi \\ M_h+M_s+M_f \end{bmatrix} \quad (1)$$

Where I_{pis} is the piston inertia about its center of mass, e_t = piston eccentricity at skirt top, e_b = piston eccentricity at skirt bottom, F_h = normal force due to hydrodynamic pressure, M_h= moment due ot hydrodynamic pressure about piston pin, F_{fh} = total hydrodynamic friction force, M_f = moment of total hydrodynamic friction force, Fs = tanØ (F_G+F_{IP}+F_{IC}) and M_s= F_GC_P - $F_{IC}C_G$.

The magnitude of the gas force is a function of crank rotation angles for the 720° cycle. The gas force magnitude profile is shown in Fig. 2 below.

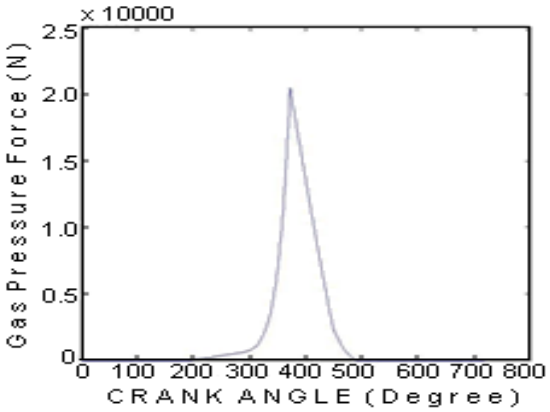

Figure 2 Gas Pressure Force Diagram [5]

4. CALCULATION OF HYDRODYNAMIC PRESSURE FORCE

The following 2-D Reynolds equation (2) is used to calculate the hydrodynamic pressures and forces [6]

$$\frac{\partial}{\partial x^*}\left(h^{*3}\frac{\partial p^*}{\partial x^*}\right)+\left(\frac{R}{L}\right)^2\frac{\partial}{\partial y^*}\left(h^{*3}\frac{\partial p^*}{\partial y^*}\right)=\frac{\partial h^*}{\partial x^*} \quad (2)$$

Where h = lubricant film thickness and p = hydrodynamic pressure. Boundary conditions to solve the Reynolds equation are as follows:

$$\frac{\partial p}{\partial x}_{x=0} = \frac{\partial p}{\partial x}_{x=\pi} = 0;$$

Where p = 0 when $x_1 \le x \le x_2$ and p(x, 0) = p(x, L) = 0

5. CALCULATION OF LUBRICANT FILM THICKNESS

The lubricant film thickness without considering the bulk elastic deformation of piston skirts is given by (3) [7]

$$h = C + e_t(t)\cos(x) + [e_b(t) - e_t(t)](y/L)\cos(x) \quad (3)$$

where C = nominal radial clearance between piston and cylinder bore.

6. VISCOELASTIC FLUID MODEL

An upper convected Maxwell model is applied to present solutions for the unsteady flow induced by a constantly accelerating plate between two side walls perpendicular to the plate and by incorporating constant density, viscosity and a small fluid relaxation time. The continuity, momentum and constitutive equations for the incompressible non Newtonian fluid flow are solved by using a regular perturbation method. Specifically, we assume an asymptotic solution in the form of a double perturbation expansion in powers of ε and De. The leading term in the conventional lubrication solution is denoted by $[\ell]$ while the two perturbation corrections are denoted by $[\varepsilon]$ and [De].

The leading term of partial derivative of pressure is obtained from the simple Reynolds equation (4).

$$\frac{\partial}{\partial x}\left(\overline{h^3}\frac{\partial p_h}{\partial x}\right)+\frac{\partial}{\partial y}\left(\overline{h^3}\frac{\partial p_h}{\partial y}\right)=6\eta U\frac{d\bar{h}}{dy} \tag{4}$$

The correction term of the pressure, (5), is obtained by taking double derivative of leading term of velocities, U, [6]

$$\frac{\partial P^{(\varepsilon)}}{\partial x}=2\frac{\partial^2 U^{(\ell)}}{\partial x^2}+\frac{\partial^2 U^{(\ell)}}{\partial y^2} \tag{5}$$

which gives to (6)

$$\frac{\partial P^{(\varepsilon)}}{\partial x}=12\left(\frac{h^3-h_m}{h^3}\right)+2\left(\frac{3h_m}{h^3}+\frac{2}{h^2}\right)\frac{dh}{dx} \tag{6}$$

For the Deborah term of pressure, P^{De}, modified Reynolds equation, (7), is solved [6], which gives,

$$\frac{\partial P^{(De)}}{\partial x}=-18\frac{{h_m}^2}{h^5}\frac{dh}{dx}+18\frac{h_m}{h^4}\frac{dh}{dx}-\frac{4}{h^3}\frac{dh}{dx}-12\frac{h_d}{h^3} \tag{7}$$

Where h_m = mean film thickness, and h_d = Deborah film thickness. Eq. (8) is the expression for Deborah film thickness

$$h_d=\left\{\frac{\frac{3}{8}\left(\frac{{h_m}^2}{{h_1}^4}-\frac{{h_2}^2}{{h_0}^4}\right)-\frac{1}{2}\left(\frac{h_m}{{h_1}^3}-\frac{h_m}{{h_0}^3}\right)+\frac{1}{6}\left(\frac{1}{{h_1}^2}-\frac{1}{{h_0}^2}\right)}{\int_0^1\frac{1}{h^3(x)}dx}\right\} \tag{8}$$

Now total pressure gradient, $\frac{dp}{dx}$, is calculated according to (9).

$$\frac{dp}{dx}=\frac{\partial P^{(\ell)}}{\partial x}+\frac{\partial P^{(\varepsilon)}}{\partial x}+\frac{\partial P^{(De)}}{\partial x} \tag{9}$$

And the resulting expression is used in the calculation of shear stress which will further give hydrodynamic friction force.

7. RESULTS AND DISCUSSION

The basic non-Newtonian hydrodynamic lubrication fluid flow model is simulated to generate the results for discussion. The generated results show the secondary eccentric displacements of the piston, hydrodynamic film thickness profiles and the pressure fields respectively.

A. Eccentricities of the piston skirts

In Figs 3, 4, 5, and 6, the profiles of E_t and E_b represent the dimensionless eccentricities of the top and bottom skirt surfaces of the piston. The E_t and E_b curves are plotted with respect to three horizontal lines i.e., the upper line, the middle line, and the lower line. The upper line and the lower line represent nonthrust and thrust sides of the liner. The middle line shows the concentric position of the piston with respect to the cylinder liner. The E_t and E_b curves are plotted against the 720° crank angle rotation. If the E_t or the E_b curve touches either the upper line at 1.0 or the lower line at -1.0, then a solid to solid contact gets established between the skirt and liner surfaces and consequently wear will take place. Piston eccentricity curves in the four speeds generally follow the same path such that initially concentric piston motion in the induction stroke, lateral eccentric displacements predetermined towards the nonthrust side during the induction, and compression strokes and speedy directional eccentric shift towards the thrust side at a piston position near the end of compression stroke.

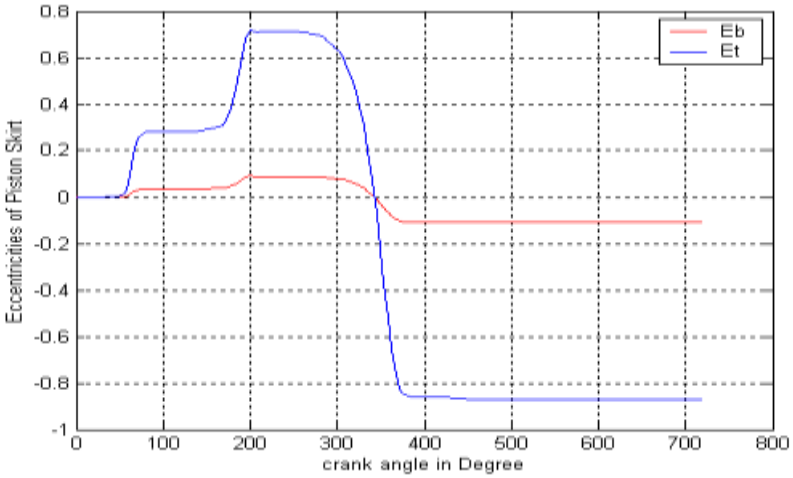

Figure 3 Eccentricities of Piston Skirts (mm) at 1000 rpm

At the engine speed of 1000 rpm, the instantaneous directional shift in the eccentric displacement of the piston skirts top surface during the compression and expansion strokes keeps a considerable distance to the lower line where it remains till the end of the exhaust stroke at 720°.

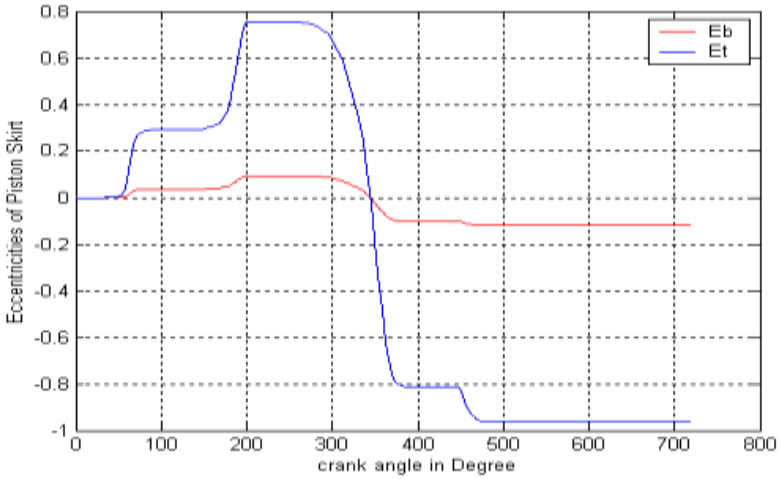

Figure 4 Eccentricities of Piston Skirts (mm) at 1500 rpm.

At the engine speed of 1500 rpm, the piston eccentricities E_t and E_b during the expansion and exhaust stroke came very close to the lower line but there is still much less possibility of solid to solid contact.

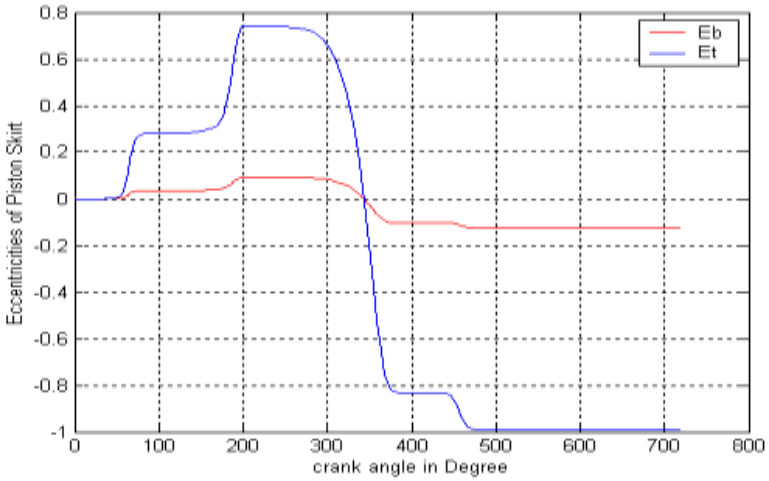

Figure 5 Eccentricities of Piston Skirts (mm) at 2000 rpm

At the engine speed of 2000 rpm, the piston eccentricities E_t and E_b during the expansion and exhaust stroke almost touched the lower line hence increasing the possibility of solid to solid contact and leading towards the piston skirt and liner wear.

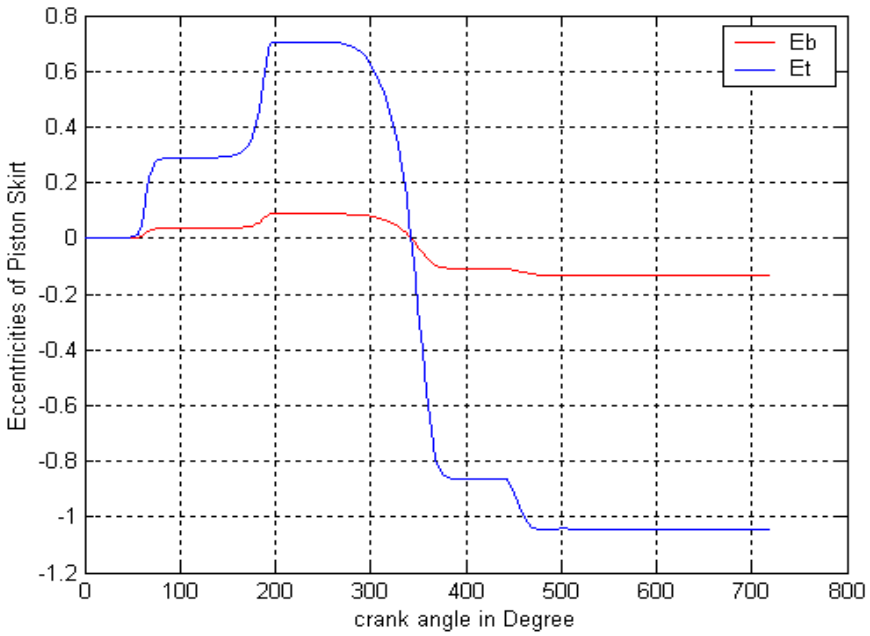

Figure 6 Eccentricities of Piston Skirts at 2500 rpm

At the engine speed of 2500 rpm, the piston eccentricities E_t and E_b during the expansion and exhaust stroke cross passed the lower line making physical contact of piston skirts with cylinder liner more certain.

B. Hydrodynamic Film Thickness

The maximum and minimum film thickness profiles as a function of 720° cycle are shown in Figs 7, 8, 9, and 10.The film thickness increases due to the eccentric displacements of the skirts before the piston completes the induction stroke. The secondary piston displacements contribute towards enhancing the film thickness. In the expansion stroke, the thrust generated by the combustion process tend to reduce the film thickness drastically. The magnitude of the maximum and the minimum film thickness profiles did not show any drastic change between the engine speeds of 1000 and 1500 rpm.

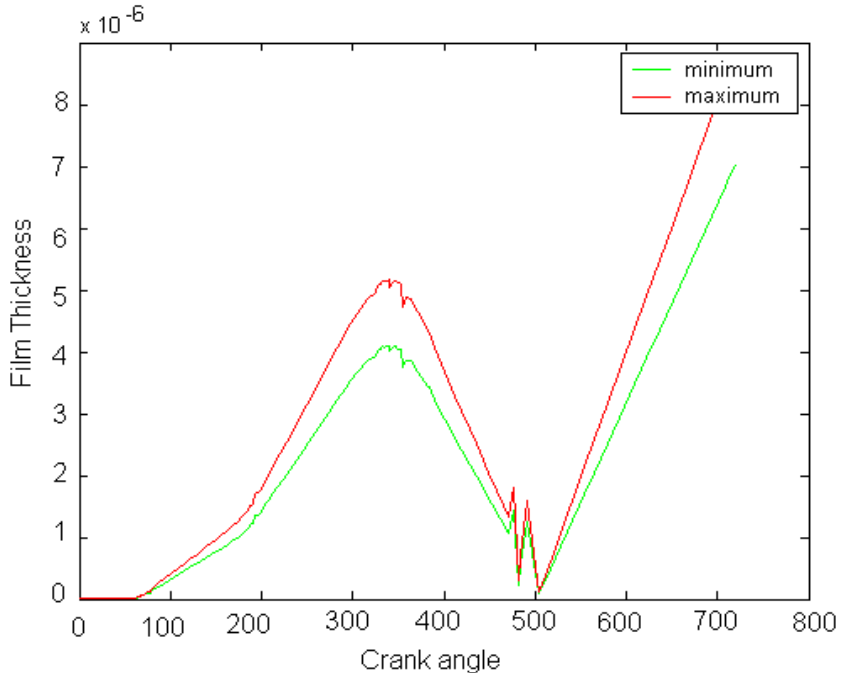

Figure 7 Hydrodynamic Film Profiles at 1000 rpm

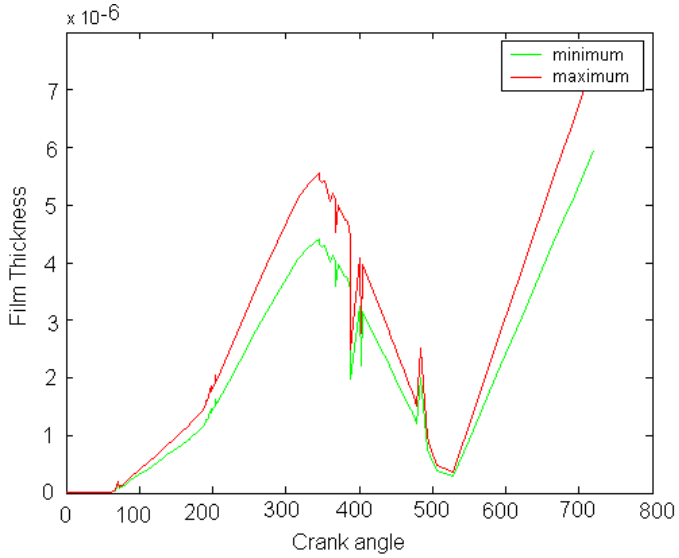

Figure 8 Hydrodynamic Film Profiles at 1500

For the engine speeds of 2000 and 2500 rpm, the decrease in film thickness was observed that highlighted the damaging effects of high engine speed at engine initial start up condition on the load carrying capacity as shown in Fig. 9 and Fig. 10.

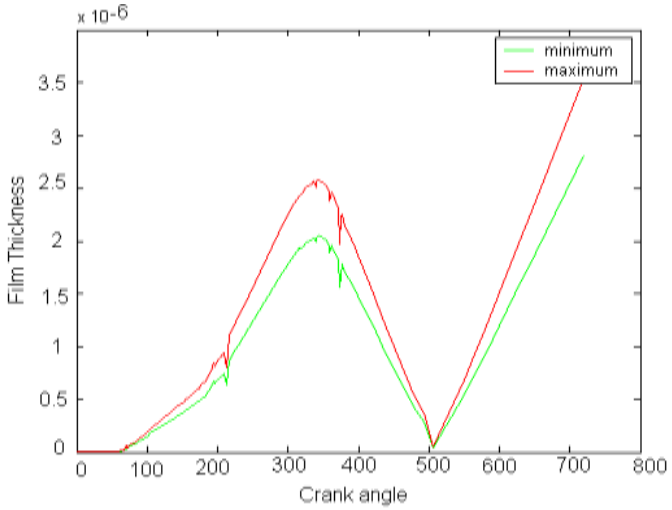

Figure 9 Hydrodynamic Film Profiles at 2000 rpm

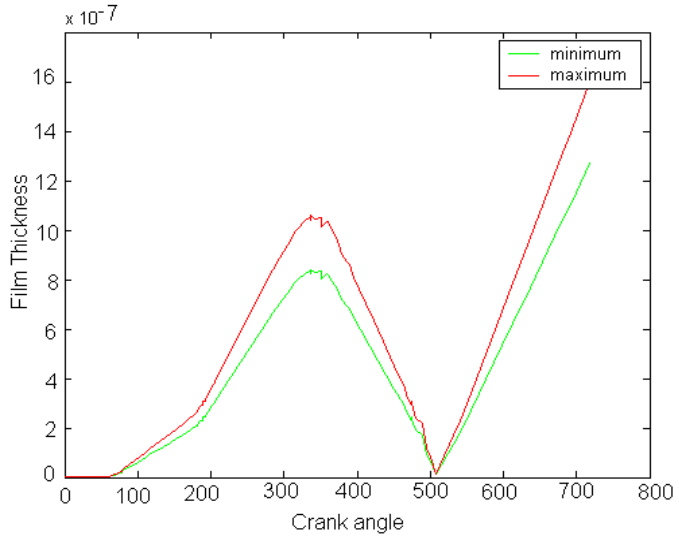

Figure 10 Hydrodynamic Film Profiles at 2500 rpm

C. Hydrodynamic Pressure fields

The hydrodynamic pressures develop over the surface of the piston skirts at each degree of piston travel. 3 dimensional pressure profiles are plotted at some of the important positions to analyze and evaluate the pressure gradient and intensities. The pressure profiles showed the same trend at 1000, 1500 and 2000 rpm as shown in Fig. 11 through Fig. 14 and pressure profiles at 2500 rpm showed zero value and hence are not plotted here.

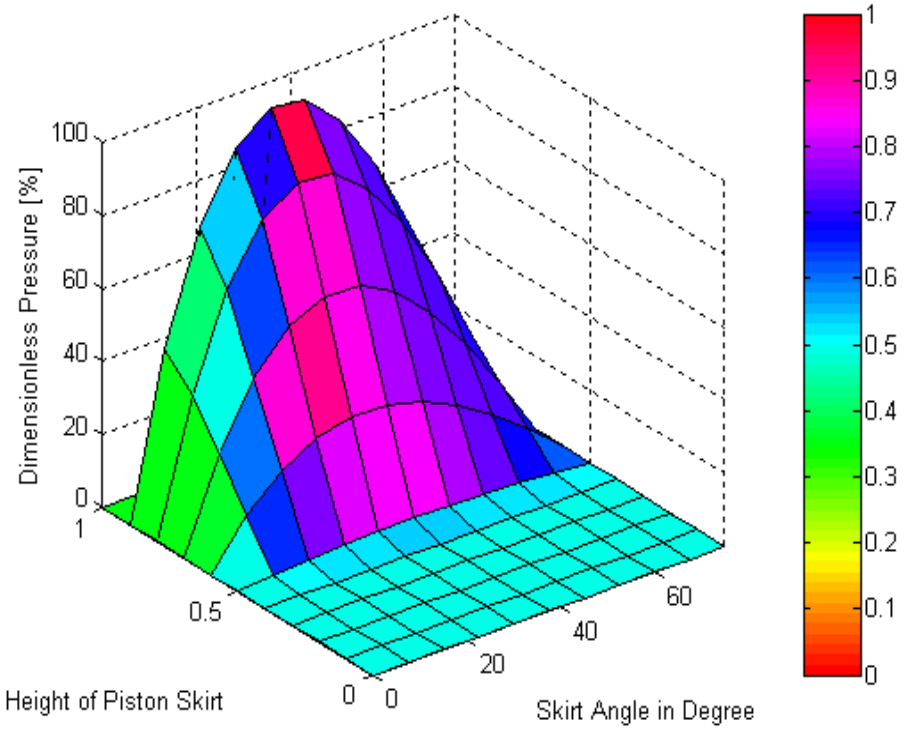

Figure 11 Pressure Profiles at 90° crank angle

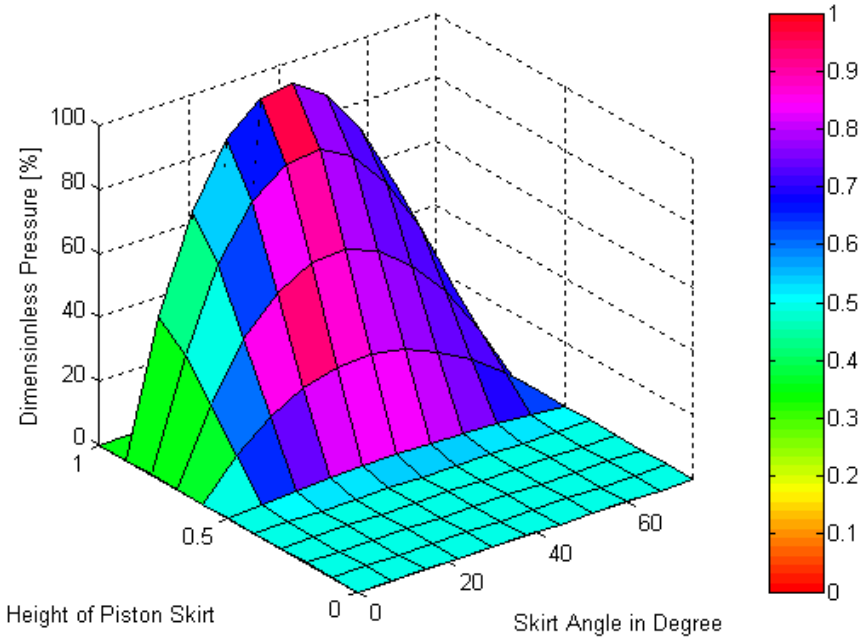

Figure 12 Pressure Profiles at 180° crank angle

In the induction stroke, the low intensity positive pressures build up gradually and are slanted towards the top surface of the skirts. Fig. 12 and Fig. 13 show gentle slopes, which indicate the rising pressures. After the mid compression stroke, the cyclic speed of the piston decreases but the gas force is still increasing.

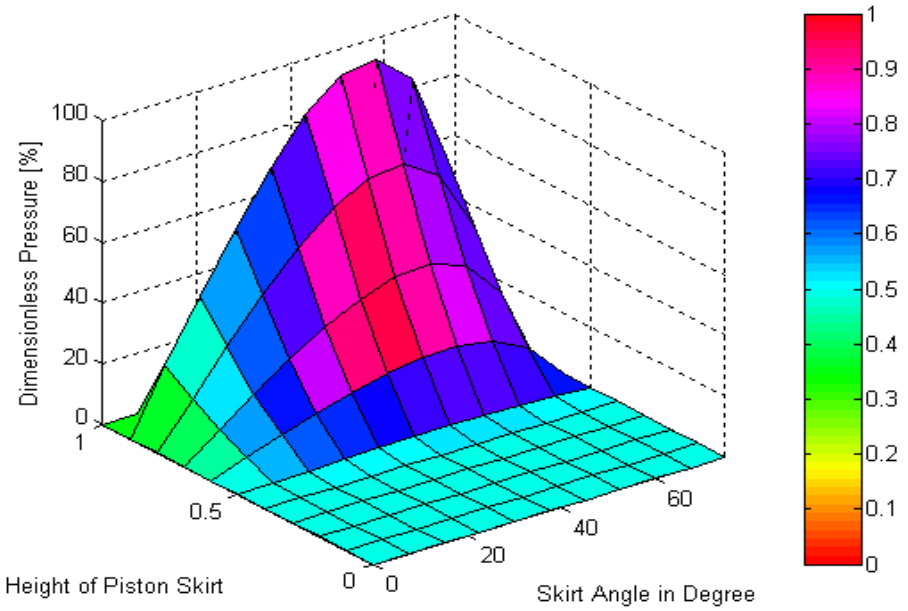

Figure 13 Pressure Profiles at 270° crank angle

The effects of moving piston inertia on the transverse side and a change in the direction of eccentric displacement vectors towards the thrust side shifts the positive pressures towards the bottom surface of the skirts as shown in Fig. 14.

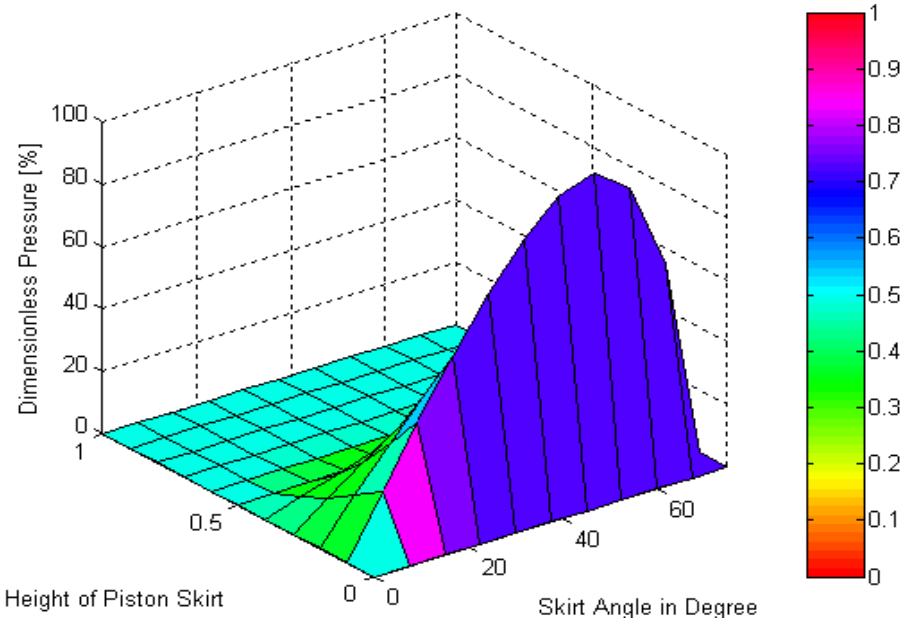

Figure 14 Pressure Profiles at 360° crank angle

CONCLUSION

A fluid flow model of 2-Dimensional non-Newtonian piston skirt hydrodynamic lubrication was developed to study the effects of medium to high initial engine start up speeds on hydrodynamic film thickness profiles. The major findings of the study are as follows:

- The initial engine start up speed at medium range, i.e. 1000 rpm, was the speed at which chances of adhesive wear of piston skirts surface were minimized due to the maximum improvement in the secondary eccentric motion of the piston. On the other hand, at the high engine speed of 2500 rpm the opposite effects were observed.
- The maximum and minimum hydrodynamic film thickness profiles are reduced considerably at the speed of 2500 rpm compared to the profiles at the speed of 1000 rpm.

In order to optimize the engine start up speed in a few initial cycles, the findings of the present study suggest that engine speeds above 2000 rpm would cause surface to surface contact and hence adhesive wear could occur which can considerably reduce the engine life. In addition, the present non-linear transient analysis agrees qualitatively with the linear analysis of the previous study by Qasim et al. [9].

ACKNOWLEDGMENT

The authors gratefully acknowledge support of Lamar University, TX, USA for Usman Chaudhri during his study at Lamar University.

REFERENCES

[1]. A.Berker, M. G. Bouldin, S. J. Kleis, and W. E. Vanarsdale, "Effects of polymer on flow in journal bearings," Journal of Non-Newtonian Fluid Mechanics, vol. 56, pp. 333-347, 1995.
[2]. P. Kumar. M. M. Khunsari, and S. Bair, "Full EHL simulations using the actual Ree-Eyring model for shear-thinning lubricants," ASME Journal of Tribology, vol. 131, pp. 108-114, 2009.
[3]. P. Yang, and S. Wen., "The behavior of non-Newtonian thermal EHL film in line contacts at dynamic loads," ASME Journal of Tribology, vol. 114, pp. 81-95, 1992.
[4]. S. J. Hupp, "Defining the role of elastic lubricants and micro textured surfaces in lubricated, sliding friction", Ph.D. thesis, Massachusetts Institute of Technology, 2008.
[5]. C. Fetecau, D. Vieru, A. Mahmood, and C. Fetecau, "On the energetic balance for the flow of a Maxwell fluid due to a constantly accelerating plate," Acta Mechanica, vol. 203, pp. 89-96, 2009.
[6]. G. W. Stachowiak and A. W. Batchelor, "Engineering Tribology," 4th ed., Elsevier, 2014, pp. 115-116.
[7]. D. Zhu, H. S. Cheng, T. Arai, K. Hamai, "A numerical analysis for piston skirts in mixed lubrication Part I: basic modeling," ASME Journal of Tribology, vol. 114, pp. 553-562, 1992.
[8]. R. Zhang, and X. K. Li. "Non-Newtonian effects on lubricant thin film flows". Journal of Engineering Mathematics, vol. 51, pp. 1-13, (2005).
[9]. S. A. Qasim, U. F. Chaudhri, and M. A. Malik, "Analyzing viscoelastic effects in pistons skirt EHL at small radial clearances in initial engine startup". Tribology International, vol. 45, pp. 16-29, 2012.